

Micro-expression spotting: A new benchmark

Thuong-Khanh Tran^a, Quang-Nhat Vo^a, Xiaopeng Hong^b, Xiaobai Li^a,
Guoying Zhao^a

^a*Center for Machine Vision and Signal Analysis, University of Oulu, Finland*

^b*School of Electronic and Information Engineering, Xi'an Jiaotong University, China*

Abstract

Micro-expressions (MEs) are brief and involuntary facial expressions that occur when people are trying to hide their true feelings or conceal their emotions. Based on psychology research, MEs play an important role in understanding genuine emotions, which leads to many potential applications. Therefore, ME analysis has been becoming an attractive topic for various research areas, such as psychology, law enforcement, and psychotherapy. In the computer vision field, the study of MEs can be divided into two main tasks: spotting and recognition, which are to identify positions of MEs in videos and determine the emotion category of detected MEs, respectively. Recently, although much research has been done, the construction of a fully automatic system for analyzing MEs is still far away from practice. This is because of two main reasons: most of the research in MEs only focuses on the recognition part while abandons the spotting task; current public datasets for ME spotting are not challenging enough to support developing a robust spotting algorithm. Our contributions in this paper are three folds: (1) We introduce an extension of the SMIC-E database, namely SMIC-E-Long database, which is a new challenging benchmark for ME spotting. (2) We suggest a new evaluation protocol that standardizes the comparison of various

ME spotting techniques. (3) Extensive experiments with handcrafted and deep learning-based approaches on the SMIC-E-Long database are performed for baseline evaluation.

Keywords:

Micro-expression spotting, benchmark, evaluation protocol

1. Introduction

Affective computing is the research field that processes, recognizes, interprets, and simulates human emotions, which plays an important role in human-machine interactions analysis. Affective computing can be related to voices, facial expressions, gestures, and bio-signal [1]. Among them, facial expressions (FEs) are certainly one of the most important channels used by people to convey internal emotions. There has been much research involved in the FE recognition topic. Several state-of-the-art FE recognition methods reported an accuracy of more than 90% [1]. Aside from ordinary FEs, under certain cases, emotions can manifest themselves in a special form which is called “Micro-expressions” (MEs). [2, 3, 4].

MEs are brief and involuntary facial expressions that occur when people are trying to hide their true feelings or conceal their emotions [5]. Research from Ekman [6] shows that MEs play an important role in psychology that helps understand hidden emotions. Spontaneous micro-expressions may occur swiftly and involuntarily, and they are difficult to be actively and willingly controlled. This characteristic of MEs allows several applications. For example, when evaluating the performance of lectures based on student’s emotions, a ME fleeting across the face can reveal the abnormal hidden emo-

tions of students. In addition to the potential applications in education, ME analysis can also be promising to be applied in other fields, such as medicine, business, and national security [2]. In business, a salesperson can use MEs to determine the customer’s true response when introducing new products. Border control agents can detect abnormal behaviors when asking questions to people. For example, the Transportation Security Administration in the USA has developed the SPOT program, in which airport staffs are trained to observe the passengers with suspicious behaviors by analyzing MEs and conversational signs [5]. In medical fields, especially in psychotherapy, the doctors can use MEs as a clue for understanding patient’s genuine feelings [2]. Therefore, ME analysis plays an essential role in analyzing people’s hidden feelings in various contexts.

Unlike regular facial expressions, which we can recognize effortlessly, reading micro-expression is very difficult for humans. It is because MEs are too short and fast for human eyes to spot and recognize. The performance of ME recognition performed by humans is still deficient even with a well-trained specialist. Meanwhile, many studies in the computer vision field have been reported the impressive performance for Facial Expression Recognition and Facial Analysis tasks [7]. Consequently, it is interesting to see how to utilize computer science, especially computer vision, for ME analysis.

The research of automatic ME analysis in computer vision is divided into two main problems: recognition and spotting. The former is the determining the emotional state of MEs, while the latter is locating the temporal positions of MEs in video sequences. Currently, most of ME research focuses on the recognition task with many novel techniques [3, 8], while ME spotting still

has limited studies. It is argued that detecting ME is probably even more challenging than ME recognition. A study in [2] reported an oblique reference for this issue in human test experiments, where the automatic ME recognition methods outperformed humans, while the accuracy is much lower when the ME spotting task is added to the ME analysis system. For real-world applications, ME positions must be determined first before any further emotion recognition or interpretation. Therefore, ME spotting is an important task in developing a fully automatic ME analysis system.

Although there is increasing attention involved in the spotting task, there are still several issues. First, the database for ME spotting is quite limited. According to the survey of [3], there are only four spontaneous databases suitable to evaluate spotting methods. Additionally, the existing ME spotting studies have been evaluated on the very limited databases. The length of videos is often 5-10 seconds that does not consist of challenging cases: eye blinking, head movements, and regular facial expressions, which are easily confused with MEs. If we consider building the real environment system of ME analysis, we need to evaluate the ME spotting methods on longer videos with more complex facial behaviors. Thus, creating more challenging databases for ME spotting is an important task. Second, it is difficult to make a fair comparison between existing techniques as they were often evaluated with different evaluation protocols. Moreover, existing evaluation protocols only focus on the correct location of spotted ME samples without considering the accuracy of detected ME intervals. Several recognition techniques require the correct location of onset/apex/offset frames for the recognition [8, 3, 9]. Recently, most ME recognition studies have been devel-

oped and experimented on manually segmented ME samples with an exactly right border, so the accuracy would largely reduce if the input ME samples contain incorrect frames. For example, in the research of Li et al. [2], the performance of ME recognition is more than 65% when evaluated on the manually processed ME samples. However, when authors evaluate their whole ME analysis system, which consists of both spotting and recognition, the performance of recognition is less than 55%. Thus, if the returned ME samples have many neutral frames or incorrect locations of apex frames, it can cause the lower performance of the recognition task. Consequently, it is meaningful to standardize the performance evaluation of ME spotting that conducts experiments under the same evaluation setting and the same metric.

Overall, to overcome the mentioned issues, we make three contributions to this work:

- We introduce a new challenging database for ME spotting, which is the new benchmark for the spotting task.
- We suggest a new set of protocols that standardize the evaluation of ME spotting methods. Our protocols aim to make a fair comparison among spotting techniques by considering both the correct ME locations and ME intervals, which are two important factors for the following ME recognition step.
- With the new ME database and the proposed evaluation protocols, we evaluate several recent ME spotting approaches, including traditional approaches and deep learning approaches, and provide baseline results for reference in future ME spotting studies.

The rest of this paper is organized as follows. The second section reviews the works related to ME spotting and databases. The third section introduces the new ME spotting database. Next, we describe the selected spotting methods which are used for providing the baseline results. Then, the proposed protocols are introduced in section 5. Finally, the last section reports experimental results and our conclusion.

2. Related Work

MEs are subtle facial emotions and low-intensity movements. Thus they are difficult for spotting by ordinary people. The spotting of MEs usually requires well-trained experts. In order to develop an automatic ME analysis system, several public ME databases and ME spotting studies have been proposed in the literature.

2.1. *Micro-expression database*

As the ME analysis research in computer vision has become an attractive topic in the last few years, the number of publicly spontaneous ME databases is still limited. In the survey of Oh et al. [3], there are only 11 databases for ME research, while most of them are only built for ME recognition. Additionally, several databases for ME spotting contain only the acted MEs which are different from the spontaneous ones thus the models built based on acted MEs would not work well in the real world application. In the case of MEs, spontaneous emotions are more genuine than acted emotions.

⁰All the baseline source codes and the dataset will be released upon the publication of this work.

Therefore, we only summarize the spontaneous databases which are suitable for ME spotting. In Fig. 1, three examples of ME samples from these spontaneous databases are illustrated.

SMIC is the first database recorded by three different types of camera: high speed (SMIC-HS), normal visual (SMIC-VIS), and near-infrared (SMIC-NIS). In 2013, Li et al. [10] also extended the SMIC by adding non-micro frames before and after the labeled micro frames to create the extended version of SMIC, namely SMIC-HS-E, SMIC-VIS-E, and SMIC-NIR-E. This dataset contains 166 ME samples from 16 subjects.

Following the previous version CASME and CASME-II, $CAS(ME)^2$ [11, 12, 13] is also extended for the ME spotting task. The $CAS(ME)^2$ database is divided into two parts: Part A contains both spontaneous macro-expressions and MEs in long videos, and Part B includes cropped expression samples with frames from onset to offset. Totally, $CAS(ME)^2$ has 194 ME samples captured from 19 subjects.

In the SAMM database [14], the authors added 200 nature frames before and after the occurrence of the micro-movement, making the spotting feasible. The SAMM is arguably the most culturally diverse database among all of the current public ME datasets. SAMM consists of 159 ME samples from 32 subjects.

The recent increasing need for data acquired from unconstrained “in-the-wild” situations have compelled further efforts to provide more naturalistic high-stake scenarios. The MEVIEW dataset [15] was constructed by collecting poker game videos downloaded from YouTube with a close-up of the player’s face. In total, MEVIEW consists of 41 videos of 16 subjects.

Overall, most of the databases are extended from the existing ones by adding neutral frames to after and before ME samples to create long videos. This approach is reasonable because recording new videos takes much effort and requires experts to label the ground truth. However, the length of extended videos is still short (5-10 seconds per video), so that they do not contain many types of other facial behaviors as in real situations. This issue prevents the development of a real-life ME spotting system. Hence, we decided to create a new ME spotting database with longer videos and more challenging cases of facial behaviors.

2.2. Micro-expression spotting

When a potential application of ME analysis is implemented in real-life, it needs to detect the temporal locations of ME events before any recognition step can be applied. Therefore, MEs spotting is an indispensable module for a fully automated ME analysis system. Several studies have been involved in this topic. In the scope of this paper, we will explore the current trend of ME spotting research in the literature.

In the beginning, almost all methods try to detect ME in videos by computing the feature difference between frames. For example, Moilanen et al. [16] spot MEs by using the Chi-Square distance of Local Binary Pattern (LBP) in fixed-length scanning windows. This method is utilized to provide the baseline results in the first whole ME analysis system, which combines spotting and recognition [5]. Patel et al. [17] proposed calculating optical flow vectors for small local spatial regions, then using heuristic algorithms to remove non-MEs. Wang et al. [18] suggested a method named Main Directional Maximal Differences, which utilizes the magnitude of maximal

difference in the main direction of optical flow. Recently, Riesz transform combining with facial maps has been employed to spot MEs automatically [19]. Kai et al. [20] proposed spotting the spontaneous MEs in long videos by detecting the changes in the ratio of the Euclidean distances of facial landmarks in three facial regions. We categorize the mentioned techniques as the **unsupervised learning** approach.

Nevertheless, the tiny motions on the face, such as eye blink and head movement, are usually very difficult to discriminate from ME samples by using the thresholding techniques. Hence, some later works proposed utilizing machine learning techniques as a robust tool to distinguish ME samples and normal facial behaviors. We categorize these methods as **supervised learning** approach. In [21], the first attempt utilizing machine learning in ME spotting was introduced. In this research, the authors employed Adaboost to estimate the probability of consecutive frames belonging to a ME. Then, random walk functions were used to refine and integrate the output from Adaboost to return the final result. Recently, for providing the benchmark to standardize the evaluation in ME spotting studies, Tran et al. [22] proposed using a multi-scale sliding-window based method for detecting MEs. This method tackles ME spotting as a binary classification problem based on a window sliding across positions and scales of a video sequence. Although studies from [21, 22] take advantage of machine learning, the performances are still not good enough. The reason is that traditional learning methods are still not robust enough to handle the subtle movements of MEs.

Recently, deep learning has been becoming a new trend in many computer vision fields that overcomes traditional approaches. Several studies started

to apply deep learning for ME spotting problem. Zhang et al. [23] firstly propose using Convolutional Neural Network (CNN) to detect the apex frame by two main steps: (1) CNN architectures are built to classify neutral frames and apex frames. (2) A feature engineering method is introduced to merge nearby detected samples. However, since this method only trains the single-image classifier, it might face false alarms in videos having macro facial expression. Tran et al. [24] proposed another deep learning-based technique by combining spatial-temporal features with the deep sequence model to compute the apex score in long videos. Their framework consists of two main steps: 1) From each position of a video, they extract a spatial-temporal feature that can discriminate MEs among extrinsic movements. 2) LSTM network is utilized to both local and global correlations of the extracted features to predict the ME apex frame score. Although impressive results were reported, this method was only evaluated on two small datasets: part A of *CAS(ME)*² and SMIC-VIS-E.

Although different techniques have been introduced for the ME spotting and some achievements have been obtained, the application to a real ME analysis system is still far away. One of the reasons is that current ME databases that are used in the development of ME spotting methods are still not challenging enough comparing to the practical situations. Most of the videos in the current ME spotting databases are 5-10 seconds short video. For real applications, we need to evaluate ME spotters on longer and more challenging videos.

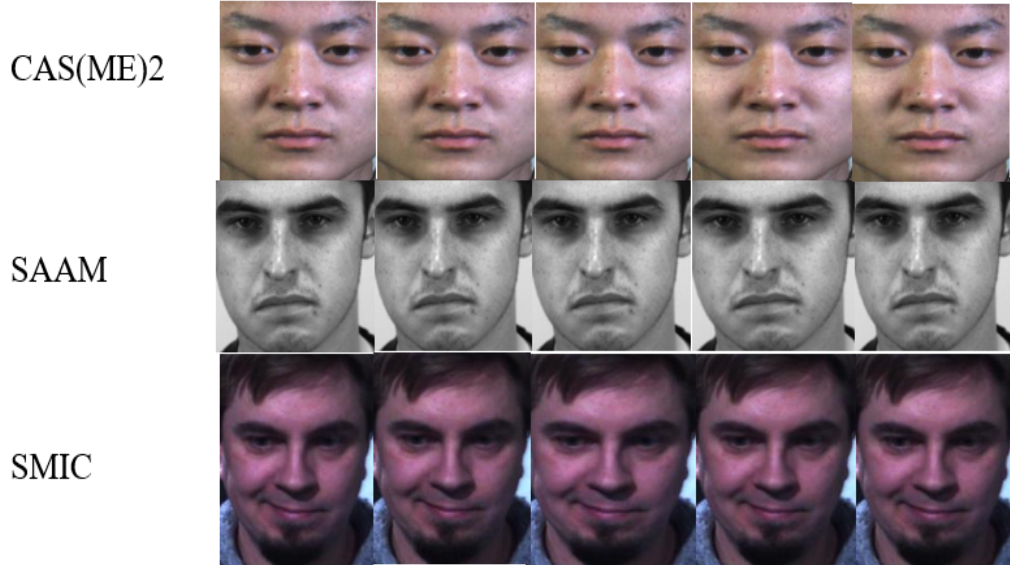


Figure 1: Examples of three ME databases for spotting. (Top) One example of $CAS(ME)^2$ displays the emotion “happines” from subject 1. (Center) The example of SAAM dataset shows the ME sample of “anger” emotion from subject 6. (Bottom) “Positive” ME sample from subject 2 of SMIC-HS dataset.

2.3. Evaluation protocols

With the significantly grown number of recent ME spotting research, there are also various evaluation metrics of ME spotting methods proposed in the literature. From the survey of Oh [3], the evaluation of ME spotting can be divided into two main approaches: ME sample spotting based evaluation and apex-frame spotting based evaluation.

Firstly, in the research of Li et al [5], the authors propose considering the spotted apex frame inside the interval $[onset - \frac{N-1}{4}, offset + \frac{N-1}{4}]$ as the true positive, where N is the length of detected window. They then plot the Receiver Operating Characteristic (ROC) curve to evaluate their methods.

Extending from ROC, Duque et al. [19] added the Area Under Curve (AUC) as the standard evaluation metric.

In the next study [21], authors still utilized the ROC curve to test their method. However, the difference is that the true positive samples are detected by the Intersection over Union (IoU) between the detected sample and ground truth. This method is formulated as:

$$\begin{aligned} \text{true positive} &: \frac{X_G \cap X_W}{X_G \cup X_W} \geq \varepsilon \\ \text{false positive} &: \frac{X_G \cap X_W}{X_G \cup X_W} < \varepsilon \end{aligned} \tag{1}$$

where X_W and X_G are spotted intervals and ME ground truth respectively, ε is set as 0.5.

In 2017, Tran et al. [22] also proposed the first version of ME spotting benchmark to standardize the performance evaluation of the ME detection task. Based on the similar protocol of object detection, they utilized the same true positive detection as Eq 1 and plotted Detection Error Tradeoff (DET) curve to compare spotters. Besides, there are also other works applying interval-based evaluation as Li et al. [5], but they proposed another performance metric such as *F1 - score* [24, 25].

Different from the above studies, instead of detecting ME intervals, several works follow the spotting of the apex frame location [26, 27]. To evaluate the performance of these methods, they selected Mean Absolute Error (MAE) to compute how close the estimated apex frames to the ground-truth apex frames are [26, 27, 3].

When performing the spotting on long videos, Liong et al. [28] introduced another measure called Apex Spotting Rate (ASR), which calculates the

success rate in spotting apex frames within a given onset and offset range in a long video. An apex frame is scored one if it is located between the onset and offset frames, and 0 otherwise. In another approach, Nistor et al. [29] proposed a combination of metrics, i.e., intersection over union percentage, apex percentage, and intersection percentage, to determine the number of correct detected apex frames.

Since there are various evaluation protocols for ME spotting, the inconsistency in comparing the performance among existing methods happens. Besides that, in the existing protocols, the evaluation between ME spotting methods still has several uncovered issues. For example, if two methods have the same number of true positive detections, there are still no metrics to determine which method is better in terms of the ME interval coverage. Therefore, it is necessary to design a standard evaluation protocol that makes a fair comparison for ME spotting methods.

3. SMIC-E-Long database

In this section, we describe our work in the construction of a new dataset for ME spotting. We realize the urgent need to explore the performance of the ME spotting task in a realistic environment. Thus, creating a new challenging database for ME spotting, which has longer videos and more complex facial behaviors, is reasonable to explore the performance of existing ME spotting techniques.

3.1. Data Acquisition

Construction of a completely new ME database often costs much effort and requires experts to label the ME ground-truth. Following the work of

SMIC-E, CAS(ME)² [10, 13], these databases are extended to enable the ME spotting by adding nature frames to before and after ME samples. However, the number of frames added to these datasets is still limited. In the construction of SMIC [30, 10], there are a huge number of neutral frames remaining from the recording step which are captured by the high-speed camera. By adding these remaining frames from the previous recording, the new dataset might contain many challenging cases such as head movements, eye blinking, and regular facial expression, which can increase potential false detections. Thus, we decide to extend the SMIC-E for creating a more challenging spotting dataset, namely SMIC-E-Long.

In the beginning, we add more than 2000 to 3000 nature frames (approximately 20 seconds) to before and after each ME sample to create longer videos (approximately 22 seconds per video). During this process, several ME samples in the original SMIC database are merged into a long video that has multiple ME samples. We also select a few clips (around 20 seconds per video) without ME samples but contain regular facial expressions that might appear in the real ME spotting situations.

Finally, our new data set is completed with 162 long videos. In Table 1, we provide the statistics of our new dataset compared with existing ME spotting datasets. There are approximately 350000 frames in 162 long videos. We have 132 long videos containing ME samples, and 25 videos have multiple MEs. There are 167 ME samples and 16 subjects in our dataset. The resolution of each video frame is 640×480 .

Comparing with existing datasets of ME spotting (in Table 1), our dataset has 162 long videos, while CAS(ME)² and SAMM have 32 and 79 videos, re-

Table 1: Comparison between SMIC-E-Long with two other ME spotting datasets

Dataset	CAS(ME) ²	SAAM	SMIC-VIS-E	SMIC-E-Long
Number of videos	87	147	76	162
Number of subject	22	20	8	16
Videos have MEs	32	79	71	132
Resolution	640 × 480	2040 × 1088	640 × 480	640 × 480
ME samples	57	159	71	166
Average time	5	10	4	22

spectively. Additionally, the average time of one video in our dataset is much longer than the existing datasets (22 Seconds compared to 5 and 10 seconds). The proposed dataset also has more challenging cases than the existing datasets. As presented in Fig. 2, we introduce other facial movements in our dataset. Two examples are presented: eye blinking and regular facial expression, which can be easily confused with MEs. As illustrated, the eye blinking only takes 12 frames, so it is similar to the characteristics of ME samples. These features make the proposed dataset more challenging than existing ones for the ME spotting task.

3.2. Face Preprocessing

At the beginning of the facial analysis system, we need to conduct the preprocessing step to align face images over video frames. This step is necessary to reduce the differences of face shapes and changes caused by big face rotation across the video.

Generic face preprocessing includes four steps: (1) Face detection and

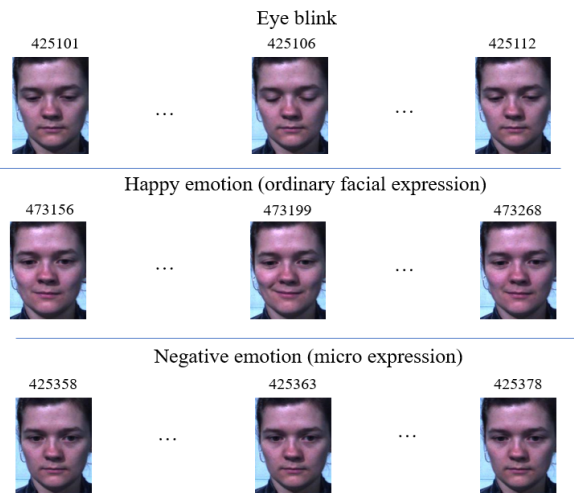


Figure 2: Example of three scenes in the new SMIC-E-Long dataset. The top case describes an example of eye blink, it takes 12 frames from frame index 425101 to frame index 425112. The middle case is the ordinary facial expression (happy emotion), it starts from frame 473156 to frame 473268. The bottom case is one example of negative emotion of ME sample which is from frame index 425358 to frame index 425378.

tracking to locate the face area across the video. (2) Landmark detection to detect the specific landmark points on the face. (3) Face registration to normalize the variations caused by the head movements and different subjects. (4) Face cropping to get the only-face area with a specific size.

In existing studies, several methods utilized various face alignment steps that make the differences in the final face size and affect the performance of the later spotting and recognition steps. For example, several methods utilized the Discriminate response map fitting (DRMF) [27, 31], while another studies select Active Shape Model [32, 21] to extract the landmark points. This issue can cause an unfair comparison of different techniques. Therefore,

we decide to carry out face-alignment for our dataset and provide the pre-processed face set that can be used as the standard input and make a fair comparison between methods.

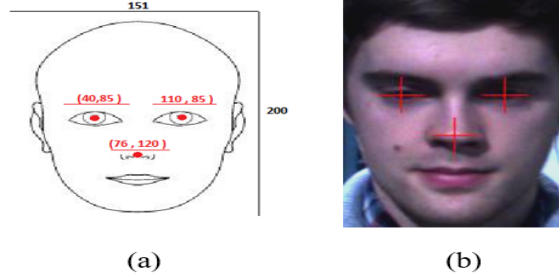


Figure 3: Illustration of template for Face-Preprocessing step. (a) The designed template when we carried out face alignment. (b) Example of SMIC frame when applying face alignment, red crosses are the markers corresponding to three points of Face Registration.

We first locate three landmark points in the first frame. Then the face registration is applied by using Local Weighted Mean [33]. The face area is cropped by using the designed template. In Fig. 3, we illustrate the designed template for face alignment. It includes three landmark points and the final face size. After detecting the landmark points in one frame, we will utilize these landmark locations in the next consecutive $M = 30$ frames for the face alignment. This is because the location of landmark points in short duration frames changes very little. For the frames with large head movements, we reduce the value of M and conduct the face alignment of the processing video again to ensure the quality of face-alignment.

4. Spotting Methods

In this section, we select various ME spotting methods from unsupervised and supervised learning approaches to provide the baseline results.

4.1. Unsupervised learning methods

4.1.1. *LBP – X^2 -distance method*

Firstly, we implement the method of Li et al. [2]. This study provides the first baseline results for ME spotting. In this method, a scanning-window with size L is stridden over video sequence. In each position, we extract LBP features from the 6×6 spatial block division at first frame (HF), tail frame (TF), and center frame (CF) of the scanning-window. Then the distance between CF and the average value of TF and HF is computed by Chi-Square distance. Finally, the threshold method is applied to return the location of the apex frame of a detected ME. Details of this method are described on [2].

4.1.2. *Main Directional Maximal Difference Analysis for spotting*

The method Main Directional Maximal Difference Analysis (MDMD) was proposed by Wang et al. [18, 34]. This method also utilizes a similar approach as *LBP – X^2 -distance method* [2] by using a scanning-window and block-based division. MDMD uses the magnitude of maximal difference in the main direction of optical flow as a feature for spotting MEs.

4.1.3. *Landmarks-based method*

We re-implement the method from [20] to explore the performance of spotting ME samples in long videos by utilizing geometric feature based on

landmark points. In this method, specific landmark points on the eyebrows and mouth areas are used to calculate the Euclidean distance ratio. A sliding window is then scanned across video frames to compute the change between the currently processing frame with the reference frame. A threshold method is used to decide which frames are MEs in the scanning window. Details of this method are described in [20].

4.2. Supervised learning method

4.2.1. Spatial-temporal feature Method

We utilize the method from Tran [22]. First, the ME samples are classified at each frame in a video sequence, then non-maximal suppression is applied to merge the multiple detected samples. Spatial-temporal features, which are widely applied in the ME and Facial Expression analysis, are extracted at each frame for the classification:

- Histogram of Oriented Gradient for Three Orthogonal Planes (HOG-TOP). This feature is extended from HOG to three dimensions to calculate oriented gradients on three orthogonal planes for modeling the dynamic texture in a video sequence.
- Histogram of Image Gradient Orientation for Three Orthogonal Planes (HIGO-TOP). Histogram of Image Gradient Orientation (HIGO) is the degraded variant of HOG. It ignores the magnitude and counts the responses of histogram bins.
- Local Binary Pattern for Three Orthogonal Planes (LBP-TOP). This feature was introduced from the work of Zhao et al. [23] as the extension

of LBP for analyzing dynamic texture. It has been widely utilized as a feature for facial-expression analysis.

We utilize SVM to distinguish the micro and non-micro samples. The details of this method can be referred to [22].

4.2.2. CNN-based method

Among deep learning structures, CNN has become popular since it offers good performance in many studies in the computer vision field. For the ME spotting, we also apply CNN as a baseline for our dataset. The proposed method is developed based on the research in [23].

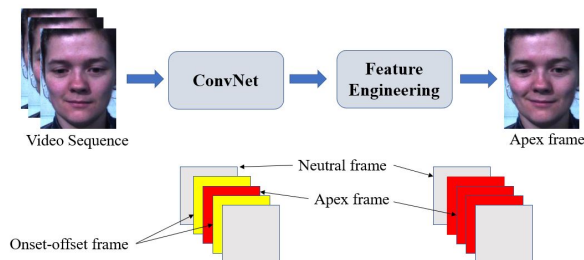


Figure 4: Overview of the ME spotting method based on CNN architectures. First, CNN models are trained to determine the neutral frame and apex frame. Then, trained models are utilized to extract features on each frame of the video. Finally, feature engineering techniques are proposed to return the final results.

As illustrated in Fig. 4, this method consists of two main components. The early step is a CNN model to distinguish the apex and non-apex frame. We consider frames from onset to offset as the apex frame to increase the number of apex frames for training. Different from the original work [23], we select two state-of-the-art CNN architectures for training the model: VGG16

[35] and ResNet50 [36]. We select these two architectures because they have been considered as the-state-of-the-art image classification methods.

The later step is feature engineering, which is used to merge the nearby detections. The features extracted from each frame of the video sequence are concatenated to construct the feature matrix F with dimension $X \times Y$, where X is the number of the frame, and Y is the length of features in the last layer of CNN models. Each row of the feature matrix F corresponds to a frame in the long video. After constructing the matrix F , we calculate the difference square sum between the values of each row with the first row. The results are concatenated to build matrix A . Then, we slide a scanning-window across positions of the matrix A with size $2 * h$ to sum the values inside the window (the result is returned as matrix B). The maximum value from the sum is considered as the apex frame. The illustration of feature engineering is displayed in Fig 5.

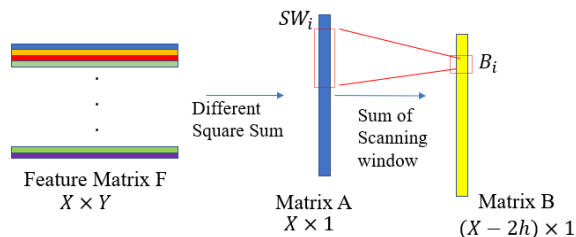


Figure 5: Illustration of feature engineering step from CNN-based spotting. X is the number of frame in one long video. $2h$ is the size of SW_i .

4.2.3. LSTM-based method

Another baseline method for ME spotting is the sequence-based learning approach proposed by Tran et al. [24]. This method includes two main steps:

feature extraction and apex frame detection based on a deep sequence model. Fig 6 presents the overview of the method.

To construct the sequence of spatial-temporal feature vectors, we slide a scanning-window across all temporal positions of a video. In each position, for example at frame i , we extract features in the sequence from frame i to $(i + L)$. By using this strategy, we consider each position is a ME candidate. In [22], the authors proposed the continuous ground truth score for each sample. However, we ignore these scores and consider that one sample is either ME or non-ME. That means, if one position is considered as a ME sample, the ground truth is set as 1, otherwise 0. For the spatial-temporal features, we utilize two kinds of features: *HIGO – TOP* and *HOG – TOP* [2].

For the apex frame detection, we employ the Long short-term memory (LSTM) network, which is a special kind of Recurrent Neural Network (RNN). It was introduced by Hochreiter [37], and was refined and popularized in many research works, especially in sequence learning. The power of the LSTM network in learning and modeling sequence data is useful for estimating ME’s position in the video sequence.

The idea for using LSTM in ME spotting is to slide a scanning-window across the video sequence. Each scanning-window contains M spatial-temporal features corresponding to M temporal positions. The constructed network inputs M spatial-temporal features and predicts M values representing the score of MEs at each temporal position. The feature at positions (i^*) that has the highest score inside a scanning window and larger than a threshold is considered as a ME sample. The specific apex frame is determined by the

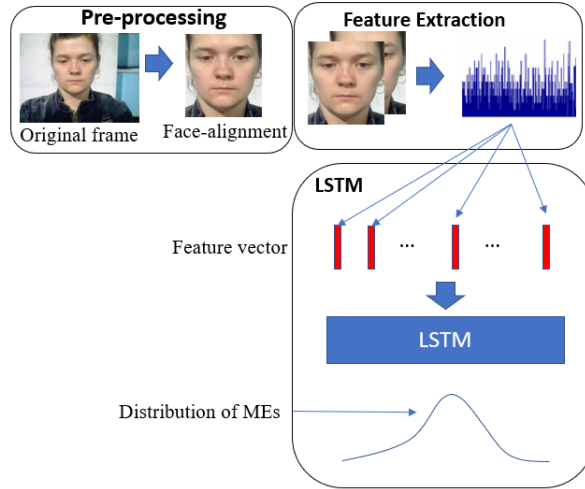


Figure 6: Overview of LSTM-based method for ME spotting. First, we extract spatial-temporal feature at each temporal position i of a video sequence. Each feature vector takes information of L -consecutive frames from the temporal location i to $i+L$. After extracting features, we slide a scanning window across video to create a sequence of features for the LSTM model. In each scanning-window, we predict the score of a candidate ME sample.

middle location $\frac{i^*+(i^*+L)}{2}$ of feature.

When dealing with ME spotting in the long videos, most of the methods utilize the scanning-window to spot ME samples. Therefore, after predicting the ME score in each frame, we need to merge the nearby detected samples using the same feature engineering strategy of the CNN-based spotting method.

5. Proposed evaluation protocol

As mentioned in the related work section, there are various performance evaluation protocols proposed in several existing research works. It is difficult to say which one is better for the ME spotting. To standardize the per-

formance comparison, we recommend a new set of protocols which is more generalized and suitable for the evaluation of ME spotting. Our proposed protocols will be described in the next sub-sections: (1) The experiment setup for splitting the data into the training and testing set. (2) The metric for evaluating the performance of spotting techniques.

5.1. Training and testing set

To split data into training and testing sets, we select Leave-one-subject-out (LOSO) cross-validation. LOSO is a common training setup that is widely utilized in ME analysis and facial expression recognition problems [2, 24, 38]. Particularly, in this method, the videos and samples belonging to one subject (participant) are kept for testing, while the remaining samples are used for training.

5.2. Performance Evaluation

For standardizing the performance evaluation of ME spotting methods, we propose two new ME movement spotting-based evaluation metrics: sample-based and frame-based. The evaluation using single apex frame detection, which is usually employed in previously proposed evaluation protocols, is not considered in our protocol. We argue that the information of a single detected apex frame is not sufficient enough for the following ME recognition step since most of ME recognition methods often require the correct extraction of the ME interval. Therefore, we want to focus on the evaluation metric that focuses on the correctly detected ME interval as well.

5.2.1. Sample-based evaluation

In this section, the sample-based evaluation metric for detected ME samples is introduced. First, we present how to decide one spotted interval is a true positive or false positive. In many ME spotting methods, the Intersection over Union (IoU) is a common approach that tackles the ME spotting as an object detection problem. This method is applied to the ME spotting task by considering the overlap between ME samples and spotted intervals (it is similar to comparing the boundary box of detection with ground truth in object detection problem [39]). The decision condition is shown in Eq. (1). The value of ε is set as 0.5 in most of the studies. It is arbitrary but reasonable. Then, we utilize the the same evaluation metric in the study of Li et al. [32] to compare the spotting methods.

To provide a more informative comparison, we also present the results of several methods following the DET curve evaluation protocol utilizing in research of Tran et al. [22]. Following Tran et al. [22], we create the Detection Tradeoff Error (DET) curve to plot the values False-Positive Per-video (FPPV) versus Miss rate. The values FPPV and Miss rate are calculated by Eq. 2:

$$\begin{aligned}
 FPPV_{OverAll} &= \frac{\sum_{j=1}^{16} FP_j}{V} \\
 MissRate_{OverAll} &= 1 - \frac{\sum_{j=1}^{16} TP_j}{N^+}
 \end{aligned}
 \tag{2}$$

where N^+ is the number of ME samples in our dataset. $V = 162$ is the number of long video in our database.

Nevertheless, the use of IoU has a drawback caused by different lengths of

ME samples in our database that have diverse lengths from 10 to 51 frames. Therefore, several ME samples can be missed by the fixed-length detected window, which is usually implemented in previous ME spotting approaches [21, 24]. For example, if we set the detected window length as 35, ME samples having a size from 11 to 17 will be missed by the evaluation based on IoU with threshold 0.5. Therefore, we define a new evaluation metric for the detected sample as follows. In the first step, we define three values for comparison as: “Hit” (TP), “Miss” (FN) and “False” (FP). “Hit” is counted when a ME ground truth has the center frame (C_{gt}) satisfies the condition with nearest detected window: $|C_w - C_{gt}| \leq 0.5 * L_{gt}$, where C_w, C_{gt} are the center location of detected window and ground truth, respectively, and L_{gt} is the length of detected ground truth. Otherwise, the un-spotted ground truth is counted as one “Miss”. “False” is counted when one detected window has the nearest ground truth satisfying the condition $|C_w - C_{gt}| > 0.5 * L_{gt}$. In Fig 7, we illustrate the examples of TP sample, FP sample and FN sample.

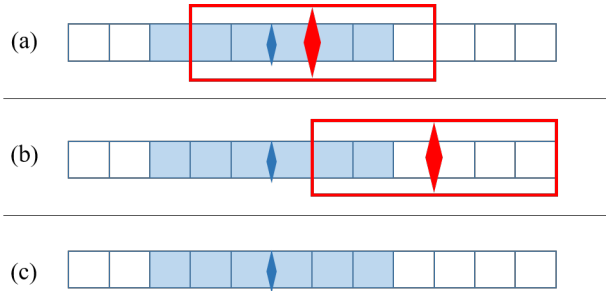


Figure 7: Illustration of detected sample and ground truth. (a) is the example of one hit. (b) is the example of one false positive and (c) is the example of one miss with no detected sample.

After calculating three values TP, FP, and FN, we need to consider two

issues regarding the F-measure values. The first one is missing of ME in the ground truth or no ME samples detected. This problem causes the division by zero in the computing of Recall and Precision. The second issue is the difference in the number of videos from each subject. Several subjects only have 4 to 6 videos. If we calculate the average value of 16 folds (corresponding to 16 subjects), it will cause the unbalance in the contribution of each subject to the final performance. To resolve these issues, at every LOSO testing fold, we integrate all tested videos into a single long video. After that, the values of TP, FP, and FN obtained in each testing phase are cumulated to calculate the (overall) Precision, Recall, and F1-score of the entire database. Then, we calculate the Precision, Recall, and F1-score following Eq. 3:

$$\begin{aligned}
 Precision &= \frac{TP_{all}}{TP_{all} + FP_{all}} \\
 Recall &= \frac{TP_{all}}{TP_{all} + FN_{all}} \\
 F1 - score &= \frac{2 * Precision * Recall}{Precision + Recall}
 \end{aligned} \tag{3}$$

where $TP_{all} = \sum_{i=1}^V TP_i$, $FP_{all} = \sum_{i=1}^V FP_i$, and $FN_{all} = \sum_{i=1}^V FN_i$ are the cumulative values of TP,FP and FN at each testing phase, respectively. V is the number of video. TP_i , FP_i and FN_i are the number of true positive, false positive and false negative frames in i^{th} video .

5.2.2. Frame-based evaluation

In the previous sub-section, we described the performance evaluation based on detected ME samples. The sample-based evaluation is a common approach when evaluating ME spotting methods. It is quite similar to the

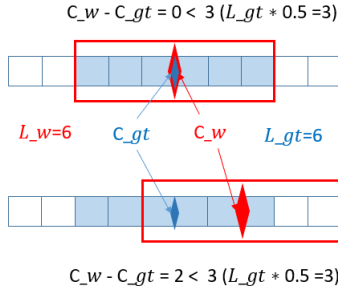


Figure 8: The limitation of evaluation by only sample-based. Both of spotters are true positive samples, but the sample-based method can not conclude the top spotter is better than the bottom spotter.

evaluation of object detection problems. However, ME spotting is a different topic with object detection. If we consider building an automatic system to detect and recognize ME in long videos, the quality analysis of detected samples should be explored. A bad detected ME sample could have too many neutral frames or miss ME frames for the next recognition task. Several recognition studies require spotted ME samples to be detected correctly (from onset - apex - offset) [5, 8, 40, 41]. Therefore, the missing of ME frames or the redundancy of non-micro frames in the spotting results can heavily affect the performance of recognition.

For addressing this issue, it is meaningful to consider the frame-based evaluation, which focuses on the correctness of spotted frames in each detected true positive sample. We complement a metric called frame-based accuracy F . The frame-based accuracy F can be defined as the mean deviation of “lengths” and “centers” of all correctly detected (TP) samples. The calculation of F is defined as Eq. 4:

$$F = \frac{1}{n} \sum_{i=1}^n \frac{(|C_{w_i} - C_{gt_i}|) + (|L_{w_i} - L_{gt_i}|)}{2 * L_{gt_i}} \quad (4)$$

where C_{w_i} and L_{w_i} are the center frame and window size of the i^{th} true positive sample. ; C_{gt_i} and L_{gt_i} are the center frame and length of ME ground truth corresponding with the i^{th} true positive sample , respectively. n is the number of true positive samples. In Fig. 8, we illustrate the effectiveness of the F metric. In this figure, we can conclude that the top spotter of the detected window is better than the bottom detector. Smaller F value means more accurately detected ME locations. To the extreme case, if all TP cases perfectly match with the ground truth, i.e., the top spotter in Fig. 8, the F is 0.

6. Experiments

6.1. Implementation

We describe here the implementation and training details of our selected baseline methods. The required development tools and the selection of important parameters will also be discussed.

First of all, to determine the value for L , the length of detected ME samples, we calculate the mean value of ME sample size. Since the mean value is 34, we set the detected window size $L = 35$. For ME spotting methods that return only the location of apex frames, such as the MDMD method, $[\frac{L}{2}]$ frames after and before the spotted apex frame are considered as inside the ME samples.

Next, we explain the implementation of each method. Firstly, we consider unsupervised learning methods. In the $LBP - X^2$ -distance method [2], the

authors did not carry out the spotting on the aligned faces. However, we conduct our experiment on the pre-processed face. For extracting the LBP feature, we utilize the **scikit-image** with the default setup [42].

With the method MDMD, we utilize the source code provided by the authors. In the original source code, the *MDMD* method outputs only the locations of apex frames. Since some detected apex frames are very close to each other, there are the overlaps of extracted ME samples. To guarantee consistency with other baseline methods, we carry out the Non Maximal Suppression (NMS) to keep only one detected ME sample in every L continuous frames. We will present the evaluation results of both the original *MDMD* method and the MDMD method with NMS (*MDMD – NMS*) in our experiments.

The landmark-based method is re-implemented by utilizing the DLIB toolbox to extract 68 landmark points for calculating the ratio between specific points. The window size of processing landmark points is also set as L .

In the spatial-temporal feature methods, we utilize the MATLAB tool provided by authors to extract three features *LBP – TOP*, *HIGO – TOP*, and *HOG – TOP* [39]. Following the research of Tran et al. [22], we only select one set of parameters: block division $8 \times 8 \times 4$, overlap 0.2, number of bin is 8. The length of images sequence for spatial-temporal feature extraction is set as L , and we employ **scikit-learn** toolbox to train the model. In this method, we also utilize the Temporal Interpolation Model (TIM) to scale the long videos into factor: 1, 0.75 and 0.5. We aim to return the adaptive size of each detected window. Three spatial-temporal feature methods are denoted

as *HIGO – TOP – SVM*, *HOG – TOP – SVM*, and *LBP – TOP* in the experiment results.

For the CNN-based methods, VGG16 and ResNet50 architectures are employed to train the neutral and apex frame classifier. We set the learning rate as 0.001, the number of epochs as 50, and the optimizer as Stochastic Gradient Descent. We denote these two methods as *VGG16* and *ResNet50* on the reported table. For the LSTM method, we set the learning rate as 0.001, and use the Adam configuration for the optimizer. The spatial-temporal features (*HIGO – TOP* and *HOG – TOP*) are extracted in the same way as in the spatial-temporal feature method. The lengths of detected ME samples and the LSTM sequence are set as L and 50, respectively. These methods are indicated as *HIGO – TOP – LSTM* and *HOG – TOP – LSTM*. Deep learning architectures are constructed by Keras framework and trained on the GPU Tesla K80 server.

6.2. Results

In this section, we present the baseline results based on our proposed evaluation protocols. We also conduct our experiment on two public datasets, CAS(ME)² and SMIC-VIS-E, to highlight the challenges of the introduced new dataset. The LOSO is used to split the dataset into the training and testing sets, as discussed in Section 5.1 and 3. Two groups of the experiment results are shown in three tables: 2, 3, and 4. Details of each set of experiments are described in the next following sub-sections.

6.2.1. Comparison on existing protocols

In this set of experiments, we evaluate the baseline methods based on the existing evaluation metrics: Precision, Recall, F1-score [32]. The results are displayed in Table 2 and Table 3. The performances of DET curve are displayed in Fig. 9,

Table 2: Experiment results on the SMIC-E-Long dataset based on the existing protocols (F1-measure with IoU).

Method	TP	FP	FN	Precision	Recall	F1-score
HOG-TOP-LSTM	55	1833	111	0.0291	0.3313	0.0535
HIGO-TOP-LSTM	31	545	135	0.0538	0.1867	0.0835
$LBP - X^2$	21	443	145	0.0452	0.1265	0.0666
MDMD	13	2934	153	0.0044	0.0783	0.0081
MDMD NMS	11	644	155	0.0168	0.0662	0.0268
Facial landmark	15	846	151	0.01745	0.0903	0.0292
HOG-TOP-SVM	11	416	155	0.0922	0.1144	0.0371
HIGO-TOP-SVM	14	857	152	0.0505	0.0602	0.0270
LBP-TOP-SVM	6	218	160	0.0267	0.0361	0.0307
VGG16	9	428	157	0.0205	0.0542	0.0298
ResNet50	11	234	155	0.0449	0.0662	0.0535

In Table 2, we can see that *HIGO – TOP – LSTM* is the best one by F1-score 0.0835. *LBP – X²* obtains the F1-score by 0.0666 in second place. In Fig. 9, we select $FPPV = 10$ as the reference point to analyze the miss rate values (lower is better). *HIGO – TOP – LSTM* is the best ME spotting

method with the miss rate of 0.681. At the same reference points, another LSTM-based method (*HOG – TOP – LSTM*) ranks second place by the miss rate of 0.721.

To demonstrate the challenge of our dataset, we provide the experimental results on the SMIC-VIS and CAS(ME)² datasets. As presented in Table 3, the performance of baseline methods on SMIC-VIS-E and CAS(ME)² is better than on SMIC-E-Long. Almost all of the F1-score values on SMIC-VIS-E and CAS(ME)² are greater than 0.3, while the performance on SMIC-E-Long shows the poor results with most of the methods having F1-score values of less than 0.1. As shown in Table 2, the number of FP samples is very high. This is because all of the baseline methods have difficulty in discriminating ME samples with other facial movements that appear more in our new dataset.

Table 3: Comparison of F1 scores between our SMIC-E-Long and two existing datasets (SMIC-VIS-E and CAS(ME)²).

Method	CAS(ME) ²	SMIC-VIS-E	SMIC-E-Long
HOG-TOP-LSTM	0.7712	0.6221	0.0535
HIGO-TOP-LSTM	0.7132	0.5532	0.0835
<i>LBP – X²</i>	0.3212	0.1245	0.0666
MDMD NMS	0.3812	0.1541	0.0268
HOG-TOP-SVM	0.3122	0.3175	0.0371
HIGO-TOP-SVM	0.3215	0.3432	0.0270
LBP-TOP-SVM	0.2856	0.3412	0.0361

Furthermore, on the SMIC-E-Long dataset, another reason for the low F1-score values is the small number of TP samples. In the final output of each spotter, we found that several ME samples can not be detected. The reason is that the ratio of ME sample size and the length of the detected samples are not suitable. As we mentioned in Section 5, ME samples having a size less than 15 can not be considered as TP if we set the length of the detection window higher than 30. Additionally, in the case of MEs with very low intensity, the ME spotters only approximately locate the apex frame inside the onset and offset of the ME interval, and hence reduce the IoU value. Therefore, it causes the missing of ME samples if we utilize the IoU to decide whether one spotted ME interval is a TP or FP. In summary, we realize that the evaluation for ME spotting that employs the IoU has a limitation caused by the diverse size of ME samples.

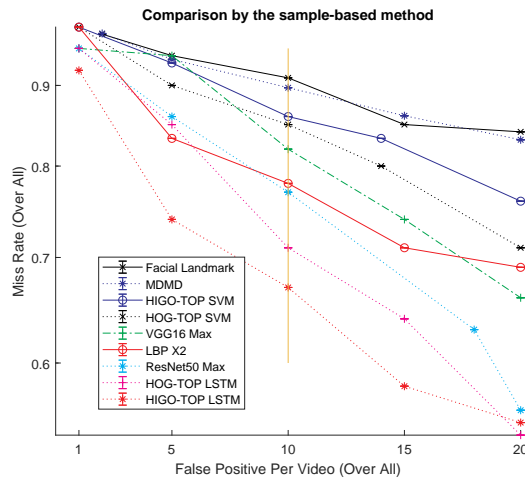


Figure 9: Performance of detectors based on interval-domain (lower is better).

6.2.2. Comparison on proposed protocol

The experimental results of selected baseline methods with the proposed protocol are shown in Table 4. In Table 4, we realize that the performance of baseline methods is increased. For example, in the results of *HIGO-TOP-SVM*, the number of TP samples is increased from 14 to 24. Consequently, the F1-score is also improved from 0.0270 to 0.0604. When analyzing the final output from each spotter, some ME samples, as discussed in the last experiment, are not correctly spotted if we utilize the IoU evaluation. In contrast, many of those samples are now considered as TP samples in our proposed protocol. It is because we do not consider the length of the detected samples in the evaluation. We only consider the center frame location of the detected window and the ME samples. Therefore, the missing of TP ME samples happens when applying IoU evaluation is now alleviated, which is fairer and more reasonable than existing evaluation metrics.

Regarding the number of TP samples, we found that *HOG-TOP-LSTM* is in the first place with $TP = 66$, and *HIGO-TOP-LSTM* is in second place with $TP = 36$. The remaining techniques return the number of TP less than 30. In the comparison by F1-score, the first place is the *HIGO-TOP-LSTM* method with F1-score by 0.0970. The second and third places are *LBP-X2* and *HOG-TOP-SVM*, respectively.

For the frame-based evaluation, F values of each baseline method are reported in Table 4. We realized that *ResNet* has the best F value by 0.1878, even though the F1-score of *ResNet* is low. By comparing four methods having the close values of TP (*HIGO-TOP-SVM*, *LBP-X2*, *HOG-TOP-SVM*, and *MDMD*), *LBP-X2* is the best detector in term

of frame coverage with $F = 0.2204$, while *HIGO – TOP – SVM* is at the second place by F value 0.2444. Based on the “ F ” metric, ME spotters can be compared more consistently in terms of the ME interval detection. It shows that the *LBP – X2* method is more sensitive to small facial changes between the apex and neutral locations, so better-detected ME intervals are obtained. On the other hand, although SVM-based methods spot ME samples with the adaptive length of detected windows, they are limited on three sizes of scale factors, while our dataset has the distribution size of ME samples ranging from 11 to 56. It causes the low “ F ” values in the SVM-based methods comparing to the *LBP – X2*. In the future study, the onset-apex-offset detection should be considered to improve the performance of the “ F ” value.

6.2.3. Discussion

In this sub-section, we analytically show the effectiveness of our selected spotting methods. Our analysis is split into four parts as following details.

Unsupervised method and supervised method. We firstly explore the effectiveness of unsupervised and supervised approaches. Based on the results of the F1-score in Table 2 and Table 4, we can observe the similar performance between two methods: the first place is *HIGO – TOP – LSTM* (a supervised method), and the second place is *LBP – X2* (an unsupervised method). However, the next places belong to supervised methods. When considering the FP values, most of the supervised methods are better than the unsupervised methods. This issue can be explained that the supervised methods have better tools to distinguish ME samples from non ME samples.

The (*LBP – X2*) method does not utilize the training term but surpasses several machine learning techniques to rank second place. Unlike other meth-

Table 4: Experiment results following our proposed protocols on the SMIC-E-Long database.

Method	TP	FP	FN	Precision	Recall	F1-score	F
HOG-TOP-LSTM	66	1930	96	0.0350	0.4216	0.0642	0.2149
HIGO-TOP-LSTM	36	540	130	0.0620	0.2108	0.0970	0.2337
<i>LBP - X²</i>	26	438	140	0.0560	0.1566	0.0825	0.2204
MDMD	24	2900	142	0.0082	0.1445	0.0155	0.7411
MDMD NMS	19	636	147	0.0290	0.1144	0.0462	0.2777
Facial landmark	20	841	146	0.0232	0.1204	0.0389	0.2236
HOG-TOP-SVM	21	406	145	0.0491	0.1265	0.0708	0.2502
HIGO-TOP-SVM	24	847	146	0.0555	0.0662	0.0604	0.2444
LBP-TOP-SVM	10	214	156	0.0446	0.0602	0.0512	0.2179
VGG16	10	427	156	0.0228	0.0602	0.0441	0.2538
ResNet50	12	233	154	0.0489	0.0722	0.0583	0.1878

ods, (*LBP - X2*) employs the adaptive threshold for each video based on the motion values. Hence, the reasons for higher performance might come from: (1) the adaptive thresholds combining with textural features are robust enough to reject the non-ME facial movements. (2) The facial actions are largely different across subjects in our new dataset. It can cause the overfitting issue in the supervised learning techniques, which decreases the performance in the testing.

Handcrafted feature and deep feature. Next, we explore the performance of supervised methods, which can be further split into two approaches: handcrafted feature learning and deep feature learning. In Table 4, an inter-

esting observation is that the use of the LSTM is not always better than the traditional machine learning techniques in term of F1-score ($HOG - TOP - SVM$ is better than $HOG - TOP - LSTM$, while $HIGO - TOP - LSMT$ achieves better performance than $HIGO - TOP - SVM$). This issue can be explained by the difference between $HIGO - TOP$ and $HOG - TOP$ features. Therefore, the correlation between spatial-temporal features and learning models is an interesting topic to explore in future research. Additionally, the number of ME samples for training is still not enough, while deep learning techniques often require a huge number of training data.

Another deep learning technique in our baseline is the CNN-based method, which has lower performance since it is hard to discriminate between micro frames and neutral frames by only using a single frame. As mentioned in the specification of the CNN-based ME spotting method, frames from onset to offset of ME samples are considered as apex-frames to train the image classification model. However, when observing a single frame, several extrinsic facial movements also have similar facial action units to ME samples. This issue makes confusion in the image classification model when discriminating ME frames and other frames containing other facial movements. Hence, CNN-based methods can detect the frames of other facial movements as ME apex frames. In general, we can conclude that the use of deep sequence learning for ME spotting is promising, but we need further improvements by increase the number of ME samples.

Appearance feature and geometric feature. In our experiments, almost methods try to spot ME samples based on the appearance features: spatial-temporal feature (LSTM-based methods and SVM-based methods),

optical flow (MDMD), texture analysis, and raw-image. We only have one method using geometric features (Facial Landmark points), but this method has lower results comparing to the appearance-based approaches. The problem of the facial landmark method is that it is developed by a rather simple idea which calculating the ratio of the distance between landmark points. Therefore, this method can not detect several ME intervals having too small movements. Especially, several ME cases only occur in the eye regions that make them similar to eye blinking actions. These cases cause missing of TP samples or triggering of false detections.

Frame-based performance Additionally, most of the spotting methods use the fixed-length detected window to return the ME intervals. This issue can increase the number of neutral or missed ME frames in the interval. In our experiments, the SVM-based methods carried out the multi-scale detection to return the adaptive-size windows. However, the performance of these methods is still low. Additionally, the “F” values are not outperformed other methods that have similar TP values. To address this issue, future research needs to consider the spotting techniques that can output the adaptive detected window or focus on the spotting of the onset and offset locations.

Through the results in Table 4, it can be seen that our new dataset is very challenging following the poor F1-score and “F” values of baseline methods. It shows that the spotting task in long videos is still a very challenging problem for future research.

7. Conclusion

In this paper, we have introduced a new challenging dataset for ME spotting. We also suggested a new set of evaluation protocols to standardize the comparison among ME spotting techniques and enable a fairer comparison. Finally, we explored various spotting algorithms from handcrafted to deep learning methods to provide the baseline for future comparison.

Following the experimental results, there are still several issues that we can improve in future works. First of all, the poor performance of deep learning techniques can be improved by applying the data augmentation to increase the number of ME samples. We can employ better deep sequence models to analyze the spatial-temporal information. Cross-database evaluation needs to be conducted to explore the generalization capability of ME spotting techniques in future research. Furthermore, the detection of the onset-offset should be included in the next study to locate the ME samples correctly. Finally, the ME recognition will be considered to create a complete benchmark for the whole automatic ME analysis system.

References

- [1] Z. Zeng, M. Pantic, G. I. Roisman, T. S. Huang, A survey of affect recognition methods: Audio, visual, and spontaneous expressions, *IEEE transactions on pattern analysis and machine intelligence* 31 (1) (2008) 39–58.
- [2] X. Li, X. Hong, A. Moilanen, X. Huang, T. Pfister, G. Zhao, M. Pietikäinen, Towards reading hidden emotions: A comparative

- study of spontaneous micro-expression spotting and recognition methods, *IEEE transactions on affective computing* 9 (4) (2017) 563–577.
- [3] Y.-H. Oh, J. See, A. C. Le Ngo, R. C.-W. Phan, V. M. Baskaran, A survey of automatic facial micro-expression analysis: databases, methods, and challenges, *Frontiers in psychology* 9 (2018) 1128.
- [4] Q. Wu, X. Shen, X. Fu, The machine knows what you are hiding: an automatic micro-expression recognition system, in: *Proc. ACII*, 2011, pp. 152–162.
- [5] X. Li, X. Hong, A. Moilanen, X. Huang, T. Pfister, G. Zhao, M. Pietikäinen, Reading hidden emotions: spontaneous micro-expression spotting and recognition, *arXiv preprint:1511.00423* (2015).
- [6] P. Ekman, Lie catching and microexpressions, *The philosophy of deception* (2009) 118–133.
- [7] S. Li, W. Deng, Deep facial expression recognition: A survey, *arXiv preprint arXiv:1804.08348* (2018).
- [8] N. Van Quang, J. Chun, T. Tokuyama, Capsulenet for micro-expression recognition, in: *2019 14th IEEE International Conference on Automatic Face & Gesture Recognition (FG 2019)*, IEEE, 2019, pp. 1–7.
- [9] Y. Li, X. Huang, G. Zhao, Can micro-expression be recognized based on single apex frame?, in: *2018 25th IEEE International Conference on Image Processing (ICIP)*, IEEE, 2018, pp. 3094–3098.

- [10] X. Li, T. Pfister, X. Huang, G. Zhao, M. Pietikäinen, A spontaneous micro-expression database: Inducement, collection and baseline, in: Proc. FG, 2013.
- [11] W.-J. Yan, Q. Wu, Y.-J. Liu, S.-J. Wang, X. Fu, Casme database: a dataset of spontaneous micro-expressions collected from neutralized faces, in: 2013 10th IEEE international conference and workshops on automatic face and gesture recognition (FG), IEEE, 2013, pp. 1–7.
- [12] W.-J. Yan, X. Li, S.-J. Wang, G. Zhao, Y.-J. Liu, Y.-H. Chen, X. Fu, Casme ii: An improved spontaneous micro-expression database and the baseline evaluation, PloS one 9 (1) (2014) e86041.
- [13] F. Qu, S.-J. Wang, W.-J. Yan, H. Li, S. Wu, X. Fu, Cas(me)²: A database for spontaneous macro-expression and micro-expression spotting and recognition, IEEE Transactions on Affective Computing 9 (4) (2017) 424–436.
- [14] A. K. Davison, C. Lansley, N. Costen, K. Tan, M. H. Yap, Samm: A spontaneous micro-facial movement dataset, IEEE transactions on affective computing 9 (1) (2016) 116–129.
- [15] P. Husák, J. Cech, J. Matas, Spotting facial micro-expressions in the wild, in: 22nd Computer Vision Winter Workshop (Retz), 2017.
- [16] A. Moilanen, G. Zhao, M. Pietikäinen, Spotting rapid facial movements from videos using appearance-based feature difference analysis, in: Proc. ICPR, 2014.

- [17] D. Patel, G. Zhao, M. Pietikäinen, Spatiotemporal integration of optical flow vectors for micro-expression detection, in: Proc. ACIVS, 2015.
- [18] S. Wang, S. Wu, X. Fu, A main directional maximal difference analysis for spotting micro-expressions, in: ACCV 2016, Springer, 2016, pp. 449–461.
- [19] C. A. Duque, O. Alata, R. Emonet, A.-C. Legrand, H. Konik, Micro-expression spotting using the riesz pyramid, in: 2018 IEEE Winter Conference on Applications of Computer Vision (WACV), IEEE, 2018, pp. 66–74.
- [20] K. X. Beh, K. M. Goh, Micro-expression spotting using facial landmarks, in: 2019 IEEE 15th International Colloquium on Signal Processing & Its Applications (CSPA), IEEE, 2019, pp. 192–197.
- [21] Z. Xia, X. Feng, J. Peng, X. Peng, X. Fu, G. Zhao, Spontaneous micro-expression spotting via geometric deformation modeling, CVIU 147 (2016) 87–94.
- [22] T.-K. Tran, X. Hong, G. Zhao, Sliding window based micro-expression spotting: a benchmark, in: International Conference on Advanced Concepts for Intelligent Vision Systems, Springer, 2017, pp. 542–553.
- [23] Z. Zhang, T. Chen, H. Meng, G. Liu, X. Fu, Smeconvnet: A convolutional neural network for spotting spontaneous facial micro-expression from long videos, IEEE Access 6 (2018) 71143–71151.

- [24] T. Tran, N. VQ, X. Hong, G. Zhao, Dense prediction for micro-expression spotting based on deep sequence model, in: Proc. Electronic Imaging, 2019.
- [25] F. Xu, J. Zhang, J. Wang, Microexpression identification and categorization using a facial dynamics map, *IEEE Trans. Affect. Comput.* (2016).
- [26] W. Yan, Q. Wu, J. Liang, Y. Chen, X. Fu, How fast are the leaked facial expressions: The duration of micro-expressions, *Journal of Nonverbal Behavior* 37 (4) (2013) 217–230.
- [27] S.-T. Liong, J. See, K. Wong, A. C. Le Ngo, Y.-H. Oh, R. Phan, Automatic apex frame spotting in micro-expression database, in: 2015 3rd IAPR Asian Conference on Pattern Recognition (ACPR), IEEE, 2015, pp. 665–669.
- [28] S.-T. Liong, J. See, K. Wong, R. C.-W. Phan, Automatic micro-expression recognition from long video using a single spotted apex, in: *Asian Conference on Computer Vision*, Springer, 2016, pp. 345–360.
- [29] S. C. Nistor, A. S. Darabant, D. Borza, Micro-expressions detection based on micro-motions dense optical flows, in: 2018 26th International Conference on Software, Telecommunications and Computer Networks (SoftCOM), IEEE, 2018, pp. 1–7.
- [30] T. Pfister, X. Li, G. Zhao, M. Pietikäinen, Recognising spontaneous facial micro-expressions, in: 2011 international conference on computer vision, IEEE, 2011, pp. 1449–1456.

- [31] Y. Han, B. Li, Y.-K. Lai, Y.-J. Liu, Cfd: a collaborative feature difference method for spontaneous micro-expression spotting, in: 2018 25th IEEE International Conference on Image Processing (ICIP), IEEE, 2018, pp. 1942–1946.
- [32] J. Li, C. Soladié, R. Séguier, S.-J. Wang, M. H. Yap, Spotting micro-expressions on long videos sequences, in: 2019 14th IEEE International Conference on Automatic Face & Gesture Recognition (FG 2019), IEEE, 2019, pp. 1–5.
- [33] A. Goshtasby, Image registration by local approximation methods, *Image and Vision Computing* 6 (4) (1988) 255–261.
- [34] S.-J. Wang, S. Wu, X. Qian, J. Li, X. Fu, A main directional maximal difference analysis for spotting facial movements from long-term videos, *Neurocomputing* 230 (2017) 382–389.
- [35] K. Simonyan, A. Zisserman, Very deep convolutional networks for large-scale image recognition, arXiv preprint arXiv:1409.1556 (2014).
- [36] K. He, X. Zhang, S. Ren, J. Sun, Deep residual learning for image recognition, in: *Proceedings of the IEEE conference on computer vision and pattern recognition*, 2016, pp. 770–778.
- [37] S. Hochreiter, J. Schmidhuber, Long short-term memory, *Neural computation* 9 (8) (1997) 1735–1780.
- [38] A. Jain Rakesh Kumar, R. Theagarajan, O. Peraza, B. Bhanu, Classification of facial micro-expressions using motion magnified emotion

- avatar images, in: Proceedings of the IEEE Conference on Computer Vision and Pattern Recognition Workshops, 2019, pp. 12–20.
- [39] P. Dollár, C. Wojek, B. Schiele, P. Perona, Pedestrian detection: A benchmark, in: 2009 IEEE Conference on Computer Vision and Pattern Recognition, IEEE, 2009, pp. 304–311.
- [40] S.-J. Wang, W.-J. Yan, X. Li, G. Zhao, X. Fu, Micro-expression recognition using dynamic textures on tensor independent color space, in: 2014 22nd International Conference on Pattern Recognition, IEEE, 2014, pp. 4678–4683.
- [41] X. Huang, G. Zhao, X. Hong, W. Zheng, M. Pietikäinen, Spontaneous facial micro-expression analysis using spatiotemporal completed local quantized patterns, *Neurocomputing* 175 (2016) 564–578.
- [42] S. Van der Walt, J. L. Schönberger, J. Nunez-Iglesias, F. Boulogne, J. D. Warner, N. Yager, E. Goullart, T. Yu, scikit-image: image processing in python, *PeerJ* 2 (2014) e453.